



**HAL**  
open science

# Synthesis of a transesterification vitrimer activated by fluorine from an $\alpha,\alpha$ difluoro carboxylic acid and a diepoxy

Florian Cuminet, Sylvain Caillol, Éric Dantras, Eric Leclerc, Sébastien Lemouzy, Cédric Totée, Olivier Guille, Vincent Ladmiral

## ► To cite this version:

Florian Cuminet, Sylvain Caillol, Éric Dantras, Eric Leclerc, Sébastien Lemouzy, et al.. Synthesis of a transesterification vitrimer activated by fluorine from an  $\alpha,\alpha$ difluoro carboxylic acid and a diepoxy. European Polymer Journal, 2023, 182, pp.111718. 10.1016/j.eurpolymj.2022.111718 . hal-03880200

**HAL Id: hal-03880200**

**<https://hal.science/hal-03880200>**

Submitted on 7 Dec 2022

**HAL** is a multi-disciplinary open access archive for the deposit and dissemination of scientific research documents, whether they are published or not. The documents may come from teaching and research institutions in France or abroad, or from public or private research centers.

L'archive ouverte pluridisciplinaire **HAL**, est destinée au dépôt et à la diffusion de documents scientifiques de niveau recherche, publiés ou non, émanant des établissements d'enseignement et de recherche français ou étrangers, des laboratoires publics ou privés.

## Synthesis of a transesterification vitrimer activated by fluorine from an $\alpha,\alpha$ -difluoro carboxylic acid and a diepoxy

Florian Cuminet,<sup>a</sup> Sylvain Caillol,<sup>a</sup> Éric Dantras,<sup>b</sup> Éric Leclerc,<sup>a</sup> Cédric Totée,<sup>c</sup> Olivier Guille,<sup>d</sup> and Vincent Ladmiral<sup>a\*</sup>

a ICGM, Univ Montpellier, CNRS, ENSCM, Montpellier, France

b CIRIMAT, Université Toulouse 3 Paul Sabatier, Physique des Polymères, 118 Route de Narbonne, 31062 Toulouse, France

c ICGM, PAC, Univ Montpellier, CNRS, ENSCM, Montpellier, France

d Institut d'Electronique et Systèmes (IES) UMR 5214, Université de Montpellier/CNRS, 34095, Montpellier, France

\*Corresponding author: Vincent Ladmiral, email: [vincent.ladmiral@enscm.fr](mailto:vincent.ladmiral@enscm.fr)

### Abstract

An  $\alpha,\alpha$ -difluorodicarboxylic acid (P-DAF) was easily synthesized in two steps from diiodobenzene and reacted with a commercial diepoxy (BDGE). The electron-withdrawing effect of the fluorinated group activated the polymerization and gelation readily happened at room temperature. After curing at 150 °C a novel dynamic material was obtained. The P-DAF/BDGE material exhibited a high gel content (94 %) and was able to flow when heated. This material could be successfully reshaped by compression molding under mild conditions (1.5 h at 150 °C). This new material demonstrates that catalyst-free transesterification vitrimers can be prepared from difunctional monomers.

### Introduction

Thermosets are polymers made of a network of covalent bonds. Thanks to this structure, they are endowed with high chemical resistance, as they do not solubilize in organic solvents, and high thermal resistance, as they do not flow upon heating.<sup>1</sup> In the current context of pursuit for greener and more sustainable polymers, thermosets are raising concerns as they cannot be easily recycled.<sup>2</sup> An answer to this issue is the use of reversible covalent bonds to prepare the network, since such bonds can be broken into reactive species able to re-associate with similar partners elsewhere in the network and form new bonds of the same nature.<sup>3-7</sup> At low temperatures, the bonds are unreactive and the network is permanent, whereas upon heating exchange reactions between reversible bonds can take place. This feature allows the polymer chains to rearrange at the local scale, and the material to flow at the macroscopic scale and be recycled. The most extensively studied chemistry for such materials is probably the Diels-Alder and retro-Diels-Alder reactions.<sup>8,9</sup> However, the dissociative nature of this reaction often induces a dramatic loss of the network integrity during the reprocessing steps.<sup>10</sup> In 2005, Bowman et al. introduced a dynamic network in which covalent bonds exchanges proceeded via an associative mechanism triggered by visible light.<sup>11</sup> In such exchange mechanisms the crosslinking density does not decrease, as a new bond is formed when another is broken, simultaneously. Thereby, the number of crosslinks remains the same even when the network rearranges. Later, in 2011, the same idea was implemented in polyester networks, using transesterification reactions triggered by heat.<sup>12</sup> The exchange reaction was promoted by a Zn<sup>II</sup> catalyst so that the rearrangements at high temperature were fast enough to induce a flow of the material. Because the viscosity of these polymers evolves linearly with temperature as silica glasses, and because they can be shaped the same way, they were called vitrimers. This discovery generated a strong emulation within the polymer scientists community, leading to the discovery of many other exchange reactions and their implementation in vitrimers: carbonates,<sup>13</sup> dioxaborolanes,<sup>14,15</sup>

olefins,<sup>16</sup> vinylogous urethanes<sup>17–19</sup> and imines<sup>20–23</sup> are just a few examples of exchangeable functions that have been reported in vitrimers thus far. The major drawback of the polyester vitrimers is the use of an external catalyst, usually  $Zn^{2+}$ , triazabicyclodecene or phosphines.<sup>24</sup> However, these catalysts are suspected to leach out of the material or to induce premature ageing upon reprocessing.<sup>25–27</sup> To overcome this issue, some strategies were developed to synthesize catalyst-free transesterification vitrimers. Hyperbranched epoxy monomers were synthesized from BADGE and a trifunctional alcohol before curing with succinic anhydride. The resulting relatively loose network and the high content of free hydroxy groups favored the mobility and the catalyst-free transesterification.<sup>28</sup> The effect of high hydroxy group concentration alone was also reported.<sup>29,30</sup> Another strategy is to embed a catalytic function in the network. For example, tertiary amines integrated in a polyester network were proved to act as an internal catalyst and activate the material flow.<sup>31</sup> Finally, the addition of activating groups in the direct vicinity of the ester links can also promote the transesterification reaction.<sup>32</sup> Oxime-esters are a representative example of this strategy.<sup>27</sup> Recently, the activation of the transesterification reaction thanks to vicinal fluorinated groups was demonstrated.<sup>33</sup> In particular, the careful design of  $\beta,\beta,\beta$ -trifluoro and  $\alpha,\alpha$ -difluoro polycarboxylic acids, from a tetrathiol and a triphenol respectively, allowed the synthesis of catalyst-free polyester vitrimers.<sup>34,35</sup> The present work aimed at the diversification of such fluorinated monomers and of the properties of the materials obtained thereof. Inspired by the work of Poutrel et al. on the synthesis of crosslinked vitrimers from a mix of diepoxides and sebacic acid,<sup>10</sup> a catalyst-free transesterification vitrimer was synthesized from a simple difunctional  $\alpha,\alpha$ -difluorodicarboxylic acid and a commercially available difunctional epoxy. The gelation of diepoxy-diacid “2+2” systems for classical thermosets is well known<sup>36</sup> and was also reported for vitrimers.<sup>10</sup> In 2+2 systems, the ring opening of the epoxy by the acid cannot explain the gelation alone. Side reactions, such as direct esterification and epoxy homopolymerization also occur as the curing is done at high temperatures, thus inducing the crosslinking.<sup>1</sup> The goal of this work is to study the feasibility of a crosslinked network at lower temperature with fluorinated dicarboxylic acids. The activation of the transesterification by fluorine is expected to be beneficial for the crosslinking density. In this context, a novel  $\alpha,\alpha$ -difluorodiacid (P-DAF) was synthesized in two scalable steps from 1,4-diiodobenzene. P-DAF was reacted with commercial butanediol diglycidylether (BDGE) to obtain an insoluble crosslinked material which resistance to solvents, mechanical properties and flow properties were studied. The P-DAF/BDGE vitrimer ability to be reprocessed was also assessed.

## Results and Discussion

### Monomer Synthesis

A novel  $\alpha,\alpha$ -difluorinated *bis*-carboxylic acid (P-DAF, Figure 1) was synthesized for the first time, following procedures described for monofunctional analogues.<sup>37,38</sup> The conditions for this reaction feature several advantages. First, the corresponding diester is synthesized in DMSO, which is a non-toxic solvent. The temperature of the reaction is 60 °C, which is relatively mild. In addition, the purification procedure is much easier and more convenient than the silica gel chromatography previously reported, especially for large-scale syntheses.<sup>34</sup> Indeed, the reaction conditions used to prepare  $\alpha,\alpha$ -difluorinated carboxylic acids from a tri-phenol induce a partial oxidation of the latter, thus requiring a purification on silica gel to obtain the pure target monomer. Here, the purification of the crude product is easily scalable, as the desired compound is isolated by a simple recrystallization in ethanol. The overall yield after the first recrystallization was 42 %. Nevertheless, this yield was improved by removing the solvent and performing a second recrystallization to reach an overall yield of 54 %. Finally, a straightforward saponification using a potassium carbonate aqueous solution in methanol led to the pure desired diacid P-DAF as a white powder, without further purification.

## Vitrimer Network Synthesis

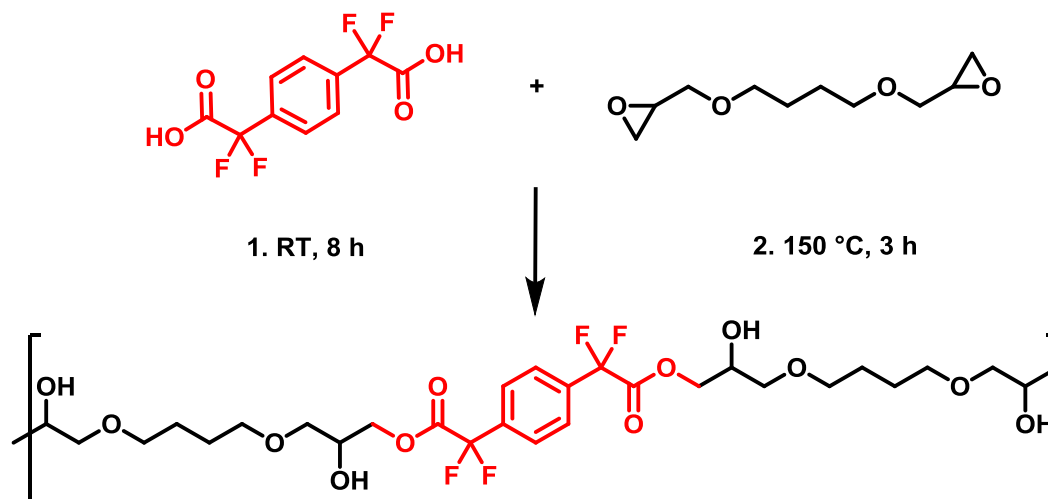


Figure 1. Vitrimer synthesis from P-DAF and BDGE

P-DAF was mixed with BDGE at room temperature (ca. 20°C) and a gel formed after after 8 h. The resulting gel was then cured at 150 °C for 3 h (Figure 1 and 3a). As previously described,<sup>34,35</sup> fluorine atoms enhance the acid reactivity towards the epoxy, allowing the ring opening to happen significantly at room temperature (RT). A FTIR monitoring was performed over the first two hours of reaction at RT (Figure S1). The shift of the acid C=O band to the ester around 1761 cm<sup>-1</sup> was too narrow to follow the conversion of these functions. Nevertheless, the intensity of the epoxy band at 914 cm<sup>-1</sup> clearly decreased over time, which indicates that the opening of the epoxy by the acid occurs at RT (Figure S2). Additionally, this reaction could also be observed using <sup>13</sup>C high resolution magic angle spinning (HRMAS) NMR spectroscopy. No deuterated solvent was used, which is common in solid state NMR, but rather uncommon for HRMAS NMR experiments. The high resolution obtained in <sup>13</sup>C allowed to acquire spectra without lock, and calibrate them using the peaks at 26 and 71 ppm of the butanediol core of BDGE. In addition, the outstandingly fast acquisition (256 scans, 0.1 s per scan) of these <sup>13</sup>C spectra allowed to qualitatively monitor the reaction by this technique. The progressive disappearance of the epoxy signals at 44 ppm (R-CH-O-CH<sub>2</sub>) and 51 ppm (R-CH-O-CH<sub>2</sub>) was easily followed over the course of 6 h, when they completely disappeared (Figures 2 and S3). Attempts to follow the reaction by <sup>1</sup>H HRMAS NMR failed because the signal resolution was too poor. <sup>19</sup>F HRMAS NMR could not be used either to follow the ester formation. Indeed the difference in chemical shifts of the α-difluoroacids and α-difluoroesters was too small (-102.1 ppm for P-DE and -103.0 ppm for P-DAF in solution <sup>19</sup>F NMR, Figures S4 and S5).

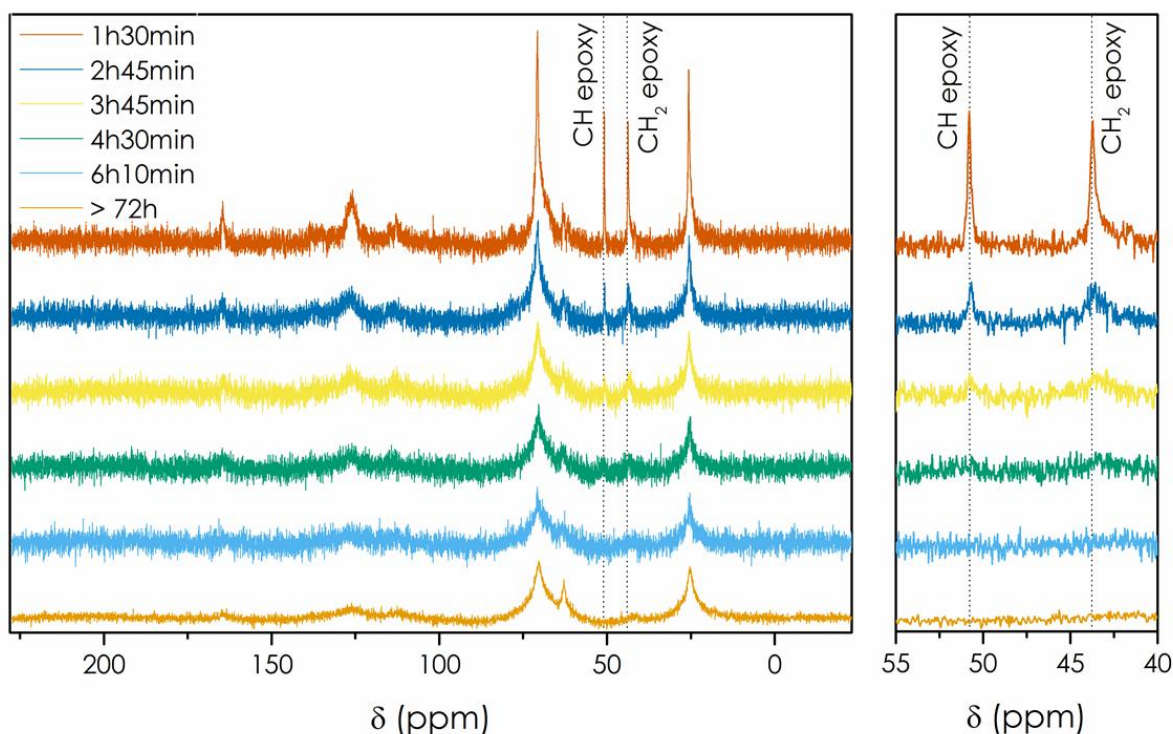


Figure 2. Monitoring of the P-DAF / BDGE polymerization reaction by  $^{13}\text{C}$  HRMAS NMR over time.

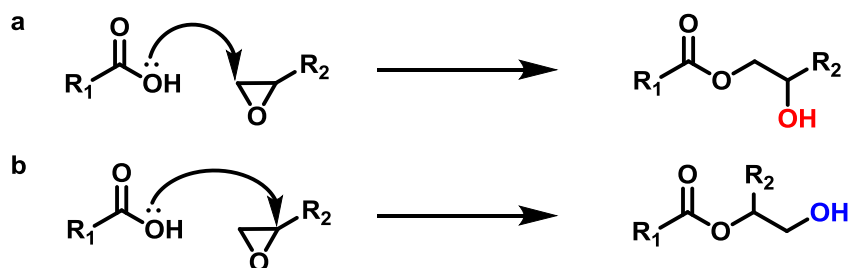
After gelation at room temperature, a DSC of the resulting material was performed to check whether the polymerization was complete. Two consecutive heating ramp from  $-100\text{ }^{\circ}\text{C}$  to  $+250\text{ }^{\circ}\text{C}$  were applied (Figure S6). On the first heating ramp a  $T_g$  is visible at  $13\text{ }^{\circ}\text{C}$ , and a small endothermic peak can be observed between the  $T_g$  and the maximum temperature. On the second heating ramp, this endothermic phenomenon is absent and the  $T_g$  increased to  $27\text{ }^{\circ}\text{C}$ . This result suggests that a curing step at higher temperature is necessary to finish the polymerization reaction. This was confirmed by the relatively low gel content observed after the polymerization at room temperature (50-60 % in polar solvents, Table S1). The end of the polymerization was also followed by monitoring the evolution of the dynamic storage modulus  $E'$  of the material with time, first at  $150\text{ }^{\circ}\text{C}$  (Figure S7) and then at  $170\text{ }^{\circ}\text{C}$  (Figure S8). At  $150\text{ }^{\circ}\text{C}$ , the storage modulus increased during 80 minutes from 0.5 to 3.7 MPa, before reaching a plateau. The analysis was stopped after 100 min. Then, a second step at  $170\text{ }^{\circ}\text{C}$  was applied, to check whether the polymerization was over or if a higher temperature would extend it again. No significant evolution of the modulus (which ranged between 4.0 and 4.5 MPa at this temperature) was observed. This result suggested that a curing step of 80 min at  $150\text{ }^{\circ}\text{C}$  was sufficient to finish the polymerization. This curing time was nonetheless doubled to ensure a complete curing; and the BDGE/P-DAF gel obtained at room temperature was cured for 3 h at  $150\text{ }^{\circ}\text{C}$ . This treatment produced a flexible light brown material (Figure 3b).



Figure 3. a. Crosslinked material after 8 h at room temperature (ca.  $20\text{ }^{\circ}\text{C}$ ); and b. after 3 h at  $150\text{ }^{\circ}\text{C}$

The swelling index (SI) and gel content (GC) of the BDGE/P-DAF material were determined in a series of solvents (Table S2). Polar solvents showed the highest affinity with the polymer, as the swelling index was 237, 148, 159 and 136 % in dimethylsulfoxide (DMSO), dichloromethane (DCM), water and tetrahydrofuran (THF), respectively. This is not surprising since the network contains many polar functions such as esters, hydroxyl and  $-CF_2$  groups. The material exhibited a gel content of 96 % in THF, thus confirming the crosslinked structure of the material. The morphology of the C=O FTIR band in the  $1780-1710\text{ cm}^{-1}$  area (Figure S9) did change after the curing step at  $150\text{ }^\circ\text{C}$ . Unfortunately, the bands of the acid and of the ester are hardly distinguishable. Nevertheless, a very weak band centered on  $2631\text{ cm}^{-1}$  which can be ascribed to the O-H stretching of carboxylic acid disappeared after the curing at  $150\text{ }^\circ\text{C}$  (Figure S10). This confirmed that a small amount of unreacted carboxylic acid remained in the material after the polymerization at room temperature. This residual unreacted  $-\text{COOH}$  groups are probably due to the lack of mobility of the reactive species after the gelation occurred.

Obtaining a crosslinked network from a difunctional epoxy and a difunctional carboxylic acid seems counterintuitive if only the reaction of epoxide opening by acids is considered. In this case, the polymerization would indeed lead to linear polymer chains and the material would be a thermoplastic. However, if other reactions happen concomitantly to the epoxy ring-opening, in particular transesterification, then 3D network can be formed.<sup>36</sup> The epoxy opening by a carboxylic acid leads to primary and secondary  $\beta$ -hydroxyl esters (Scheme 1).



Scheme 1. Epoxide opening by a carboxylic acid leads to a. secondary or b. primary  $\beta$ -hydroxyl ester.

Then, the dangling hydroxy groups can undergo transesterification with an ester of another chain/segment. This leads to crosslinks and to the formation of “sacrificial” polyol oligomers (Figure 4). This mechanism was clearly explained and theorized recently for non-fluorinated epoxy-acid vitrimers made from difunctional acids and is represented for the present system in Figure 4.<sup>10</sup>

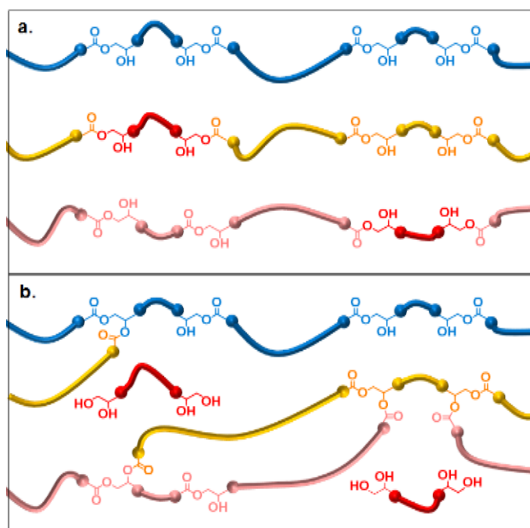


Figure 4. Expected structures of a diepoxy-diacid "2+2" polymer (a). if only epoxy opening by the acid is considered (b). if transesterification and Fisher esterification are taken into account (crosslinked network: blue, orange and pink segments and soluble sacrificial oligomers in red).

In addition, other minor side reactions could increase the degree of crosslinking of the network: 1) Fisher esterification with the remaining traces of carboxylic acid groups (Figure 5a), 2) transesterification leading to the formation of sacrificial oligomers (Figure 4), or 3) irreversible formation of ether bonds (Figure 5b).<sup>1,10</sup> Although these reactions only happen to a small extent, they generate crosslinks which can be beneficial to the formation of 3D network.

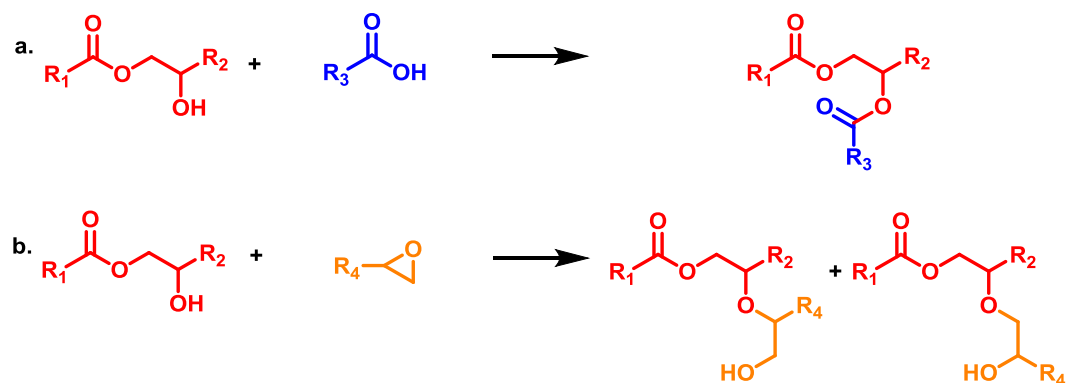


Figure 5. Possible side reactions during the curing step at 150 °C a. Fisher esterification, b. etherification by epoxy opening by an alcohol

### Vitrimer Characterization

The thermal stability of the BDGE/P-DAF vitrimer was assessed by TGA under air. The temperature of 2 % mass loss was 262 °C whereas 5 % mass loss was attained at 321 °C (Figure S11, Table 1). The  $T_g$  measured by DSC was 27 °C (Figure S6). This value is rather low considering the aromatic nature of the diacid, and shows that BDGE brings flexibility to the network, as expected. This feature also translates on the DMA experiment, with  $T_\alpha = 47$  °C. The values of the storage modulus were  $E'_G = 1.9$  GPa and  $E'_R = 11$  MPa on the glassy plateau and on the rubbery plateau respectively (Figure S12, Table 1), which is consistent with similar networks reported previously.<sup>28,29,34,39,40</sup>

Table 1. Thermal properties of the BDGE/P-DAF vitrimer

$T_{2\% \text{ loss}}$ (°C)	$T_{5\% \text{ loss}}$ (°C)	$T_g$ (°C)	$T_\alpha$ (°C)	$E'_G$ (GPa) <sup>a</sup>	$E'_R$ (MPa) <sup>b</sup>	SI (%) <sup>c</sup>	GC (%) <sup>c</sup>
-----------------------------	-----------------------------	------------	-----------------	---------------------------	---------------------------	---------------------	---------------------

262	321	27	47	1.9	11	136	96±1
-----	-----	----	----	-----	----	-----	------

<sup>a</sup> at  $T_{\alpha}$ -50 °C    <sup>b</sup> at  $T_{\alpha}$ +50 °C    <sup>c</sup> in THF

The flow properties of the BDGE/P-DAF vitrimer were studied by stress-relaxation in the time domain. To assess the role of fluorine in the flow properties, a non-fluorinated counterpart called BDGE/P-DA was prepared by reaction of 1,4-phenylenediacetic acid and BDGE at XXX °C for xxx h. A 10 % torsionnal strain was applied and full stress relaxation was observed for the fluorinated BDGE/P-DAF material at 210 °C after 45900 s (12 h 45 min, the end of the curve is noisy because of the apparatus technical limitations to keep the applied strain constant at low torque). The same experiment was performed on the non-fluorinated BDGE/P-DA counterpart. The relaxation was much slower, as only 37 % of the applied stress was relaxed after the same duration. This proves the significant effect of the  $\alpha,\alpha$ -difluoro group to activate transesterification and allow the material to flow (Figure 6).

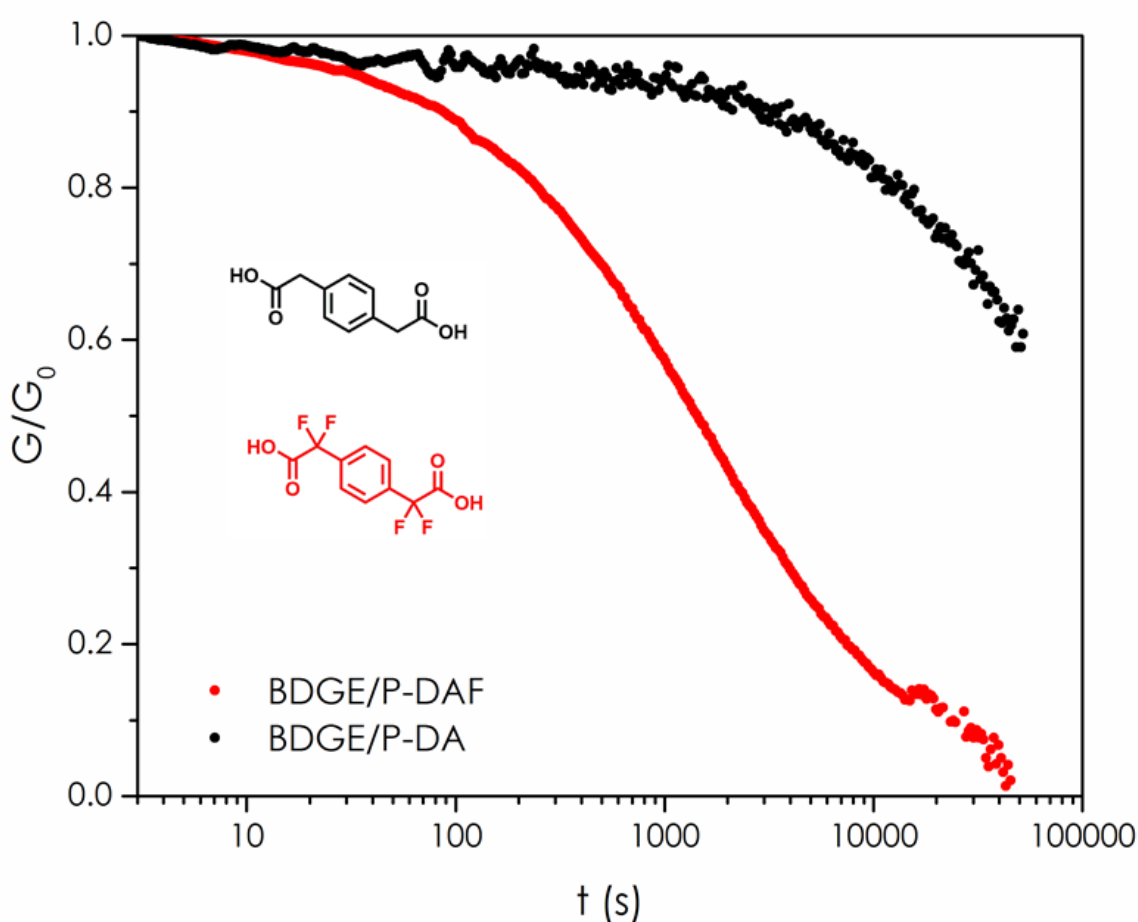


Figure 6. Stress relaxation experiments on fluorinated P-DAF/BDGE and non-fluorinated P-DA/BDGE at 210 °C with a 10 % strain.

The relaxation modulus was monitored for isotherms ranging from 170 to 210 °C (Figure 7). The stress relaxation data were fitted with a Kohlraush-Williams-Watts equation and the obtained relaxation times  $\tau_{\text{KWW}}$  were plotted in an Arrhenius diagram (Figure 7 inset). The value obtained from the curve at 170 °C was discarded, because the data at this temperature was considered inaccurate. Indeed, the relaxation seemed faster than expected compared to the other isotherms. This is likely due to a slow slipping of the sample at lower temperatures for long experiment times, in spite of the experimental efforts implemented to overcome this issue. This translates clearly on the Arrhenius

plot when the 5 isotherms values are plotted. Thus, only the isotherms from 180 °C to 210 °C were considered. The  $\tau_{KWW}$  values followed a linear fit, proving the vitrimer follows the Arrhenius law, and the activation energy was determined to be  $E_a = 118 \pm 8 \text{ kJ mol}^{-1}$  (Figure 7 inset).

hv

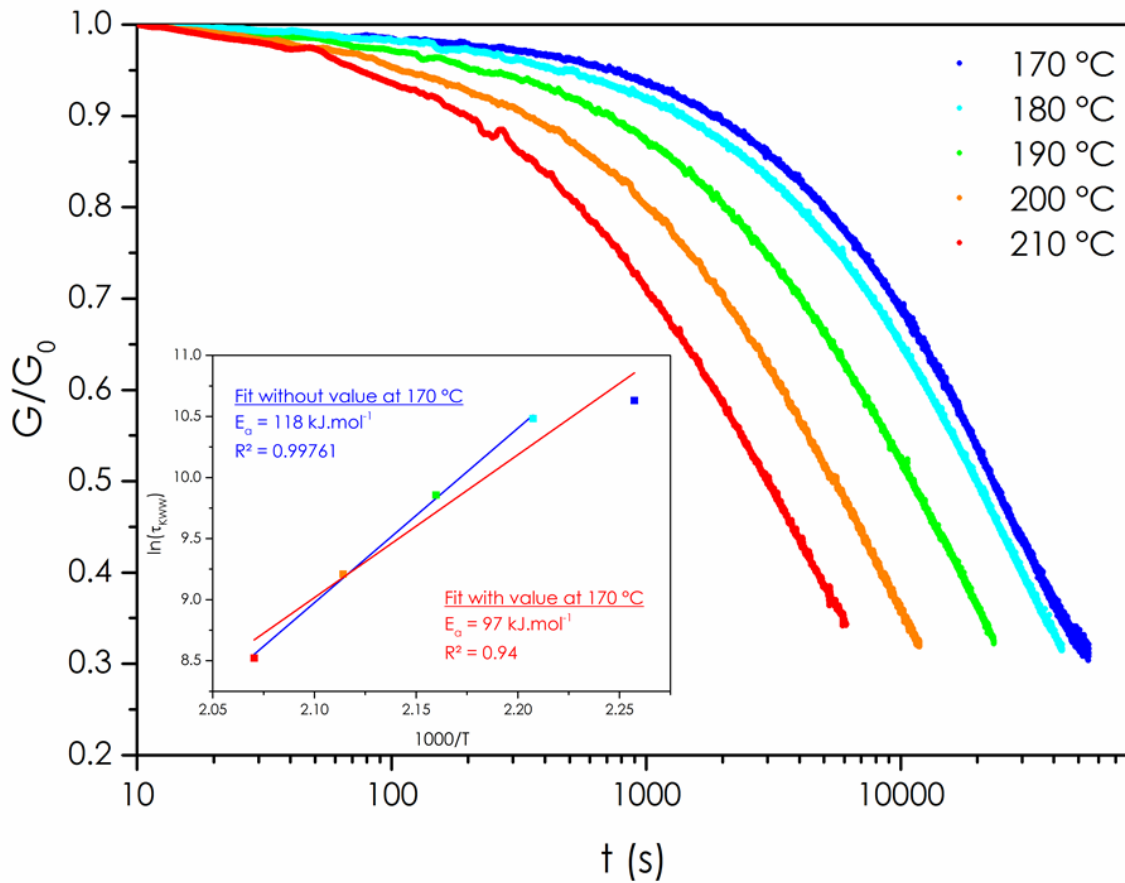


Figure 7. Normalized stress-relaxation curves from 170 to 210 °C for BDGE/P-DAF vitrimer fitted with the Kohlraush-Williams-Watts equation (KWW) and Arrhenius plot of the  $\tau_{KWW}$  relaxation times obtained.

The reprocessing ability of the vitrimer was successfully assessed by compression molding. Samples were diced into  $\approx 1 \text{ mm}^3$  pieces and reprocessed by compression molding for 1.5 h at 150 °C under a 6 ton load (Figure 8).

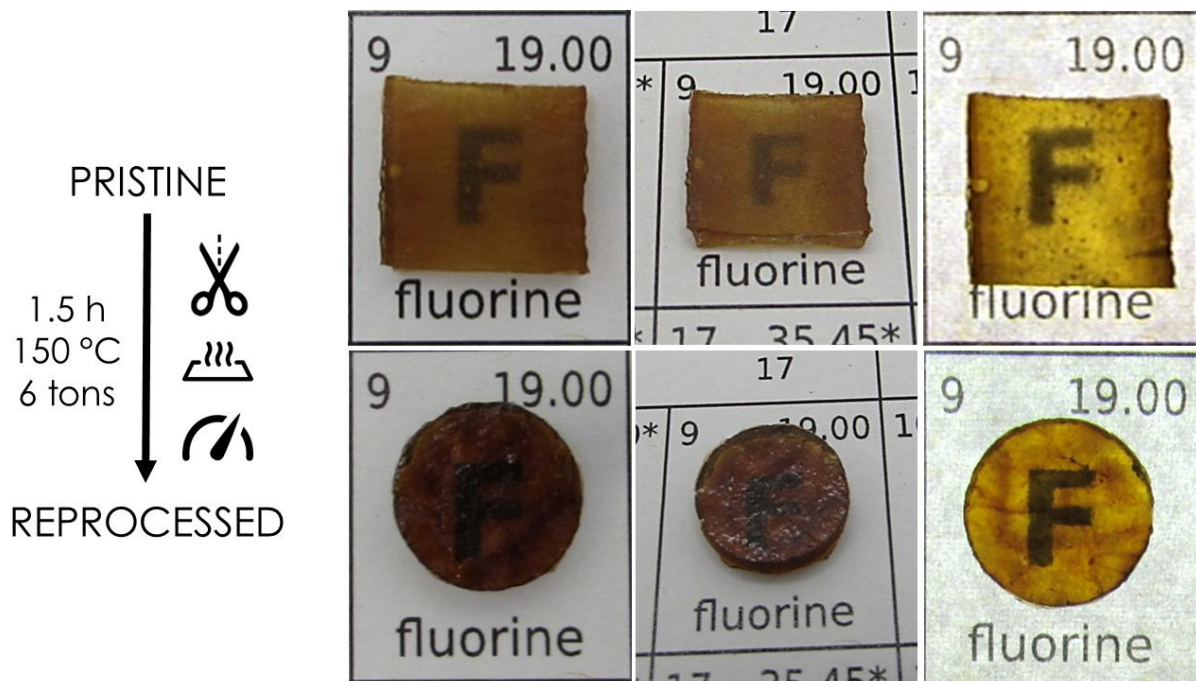


Figure 8. P-DAF/BDGE vitrimer before and after reprocessing by compression molding, front lighting (center) and backlit (right)

Table 2. Properties of P-DAF/BDGE vitrimer pristine, after reprocessing and after subsequent annealing

	Pristine	Reprocessed <sup>b</sup>	Annealed <sup>c</sup>
$T_g$ (°C)	27	-2	20
$T_\alpha$ (°C)	47	30	40
SI (%) <sup>a</sup>	136	308	-
GC (%) <sup>a</sup>	96±1	93±1	-
$E'_R$ (MPa)	11	7	6

<sup>a</sup> in THF      <sup>b</sup> 1.5 h, 150 °C, 6 tons in press      <sup>c</sup> 3 h, 150 °C in oven

The vitrimer chemical stability upon reshaping was checked by FTIR (Figure 9). A slight increase of the –OH band and the appearance of a weak band at  $1630\text{ cm}^{-1}$  were observed. These may be caused by a slight water intake of the material from ambient moisture before reprocessing. The value of  $T_g$  obtained by DSC dropped from 27 °C for the pristine material to -2 °C for the reprocessed material (Table 2 and Figure S13). The swelling index of 136 % before reprocessing increased to 308 % after reprocessing, whereas the gel content slightly decreased from 96±1 % to 93±1 % (Table 2). The water intake could lead to plasticization, or to some hydrolysis at high temperature in the heating press. By DMA the  $T_\alpha$  shifted from 47 °C to 30 °C before and after reprocessing, respectively and the modulus on the rubbery plateau decreased from 11 to 7 MPa (Table 2 and Figure S14). The  $T_\alpha$  ascribes for the effects of both plasticization and possible hydrolysis, whereas the modulus on the rubbery plateau depends only on the crosslinking density, thus the decrease observed can be ascribed to hydrolysis during reprocessing. This hypothesis of a plasticization effect after hot pressing remains plausible, as the sample is constrained between two plates which hinder water evaporation. When a reprocessed sample underwent an annealing treatment in an oven for 3 h at 150 °C, in which water is free to escape from the material, the  $T_g$  and the  $T_\alpha$  reached values ( $T_g = 20^\circ\text{C}$ ,  $T_\alpha = 40^\circ\text{C}$ ) close to those of the material before reprocessing. This results are consistent with a water plasticizing effect. Nevertheless, the modulus on the rubbery plateau was not recovered (6 MPa) which suggest partial hydrolysis. The change in the gel content, though very limited, also supports this hypothesis.

Therefore, the behaviour of the material is most likely due to a combination of both plasticization and hydrolysis (Table 2).

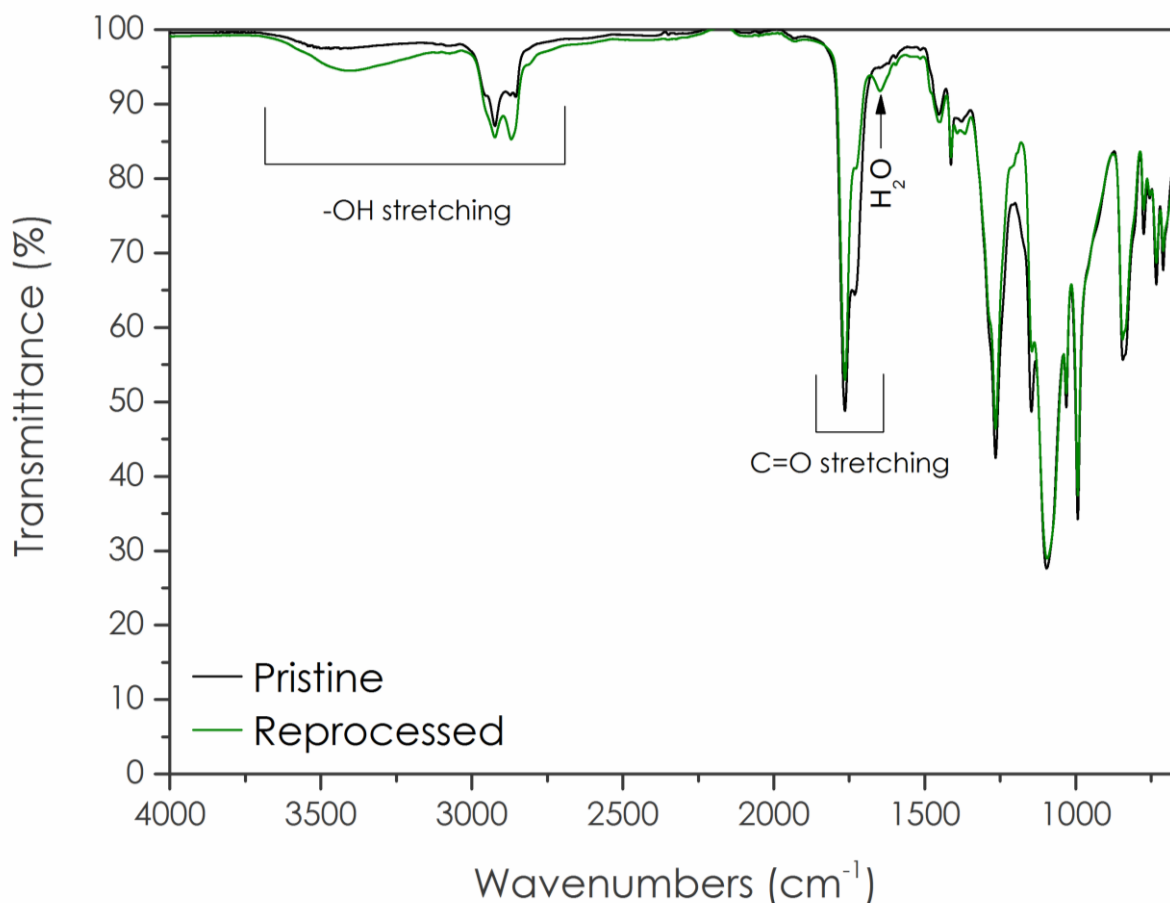


Figure 9. FTIR spectra of the P-DAF/BDGE vitrimer before and after reprocessing by compression molding

## Conclusion

Catalyst-free transesterification vitrimers were synthesized from P-DAF, an  $\alpha,\alpha$ -difluorodicarboxylic acid and a commercially available diepoxy. P-DAF was easily synthesized in two steps and purified by recrystallization. The  $\alpha,\alpha$ -difluoro groups proved to activate P-DAF reactivity towards epoxy ring opening, as the reaction with the diepoxy BDGE readily happened at room temperature. This bulk polymerization resulted in a gelled material. After completion of the curing at 150 °C for 3 h, an insoluble thermosetting material was obtained. Transesterification concomitant to the epoxy-acid reaction during the curing was responsible for the crosslinking of the network. The P-DAF/BDGE material relaxed stress when a constant strain was applied at temperatures ranging from 170 to 210 °C. The dynamic properties of this material are due to bond exchanges by transesterification activated by the inductive effect of the  $\alpha$ -CF<sub>2</sub> groups to the ester bonds. The relaxation times at different isotherms followed the Arrhenius equation, which is consistent with the behavior of a vitrimer. The P-DAF/BDGE vitrimer was then successfully reprocessed by compression molding for 1.5 h at 150 °C under a 6-ton load to give homogeneous reshaped samples, without the need for any added catalyst. The feasibility of such  $\alpha,\alpha$ -difluoro activated vitrimers from difunctional monomers will simplify the synthesis of other similar materials, as difunctional species are more available than tri- or tetra-functional ones. This could benefit in the future to a better understanding of the structure/properties relationship in such materials, but also to their potential synthesis on larger scales.

## Experimental Section

### Materials

Copper powder (Aldrich, 99 %), 1,4-diiodobenzene (Fluorochem, 98 %), 1,4-butanediol diglycidyl ether (BDGE, Aldrich,  $\geq 95$  %), 1,1,1-Tris(4-hydroxyphenyl)ethane ("TPE", Sigma-Aldrich, 99 %), 1,8-Diazabicyclo(5.4.0)undec-7-ene (DBU, Fluorochem, 98 %), ethyl bromodifluoroacetate (Fluorochem, 98 %), 1,4-phenylenediacetic acid (ABCR, 97 %) were used as received. Solvents were supplied by VWR Chemicals. Deuterated solvents were supplied by Eurisotop (99.8 %).

### Synthetic Procedures

**Synthesis of diethyl 2,2'-(1,4-phenylene)bis(2,2-difluoroacetate) (P-DE):** 1,4-diiodobenzene (41.3 g, 125 mmol, 1 equiv.) was dissolved in DMSO (300 mL) in a 500-mL round-bottom flask. Copper powder (42.17 g, 664 mmol, 5.3 equiv.) was added under vigorous stirring to obtain a suspension. Ethyl bromodifluoroacetate (51.0 g, 251 mmol, 2 equiv.) was then added. The flask was sealed with a septum and heated to 60 °C for 7 hours. The crude mixture was cooled to room temperature, poured in a mixture of ice and saturated ammonium chloride aqueous solution (1.5 L) under vigorous magnetic stirring. The aqueous solution was extracted 4 times with ethyl acetate (4 x 500 mL). The combined organic layers were washed 4 times with saturated aqueous ammonium chloride (4 x 400 mL) and twice with brine (2 x 400 mL), dried with  $\text{MgSO}_4$  and concentrated under reduced pressure. The solvent was removed under high vacuum to afford 38 grams of an orange solid-and-oil mixture. The crude product was taken in a minimum of cold ethanol, inducing a crystallization of 17 grams of the pure diester (white solid, 42 %). The filtrate was concentrated under reduced pressure and the same operation was repeated to afford another 4.9 grams of the diester (off white solid, 12 %).  **$^1\text{H}$  NMR 400MHz DMSO- $d_6$  (Figure S15):**  $\delta$  (ppm) 7.80 (s, 4 H, aromatic protons), 4.31 (quad, 4 H,  $\text{CH}_2$ ), 2.50 (DMSO), 1.21 (t, 6 H,  $\text{CH}_3$ ).  **$^{19}\text{F}$  NMR 377 MHz, DMSO- $d_6$  (Figure S16):**  $\delta$  (ppm) -102.1.  **$^{13}\text{C}$  NMR 101 MHz, DMSO- $d_6$  (Figure S17):**  $\delta$  (ppm) 163.2 (RCOOR,  $J_{\text{C-F}} = 36$  Hz), 135.4 ( $\text{C}^{\text{V}}$  aromatic,  $J_{\text{C-F}} = 26$  Hz), 126.6 (CH aromatic,  $J_{\text{C-F}} = 6$  Hz), 113.3 ( $\text{CF}_2$ ,  $J_{\text{C-F}} = 252$  Hz), 64.2 ( $\text{CH}_2$ ), 40.0 (DMSO), 14.0 ( $\text{CH}_3$ ). **HRMS (ESI+)** Calc. for  $[\text{M}+\text{H}]^+$  323.0901, found 323.0902. **FTIR spectrum:** Figure S18.

**Synthesis of 2,2'-(1,4-phenylene)bis(2,2-difluoroacetic acid) (P-DAF):** In a 250-mL round-bottom flask, 9.4 g of diester P-DE were dissolved in 80 mL of methanol. Then, 80 mL of a 1M potassium carbonate aqueous solution was added under magnetic stirring and the reaction was left to proceed overnight at room temperature. The crude mixture was then precipitated in 300 mL of 1M HCl, extracted with ethyl acetate (3 x 200 mL), washed twice with brine (2 x 150 mL), dried over  $\text{Na}_2\text{SO}_4$  and the solvent was removed under reduced pressure to afford 7.7 g of the pure diacid (white solid).  **$^1\text{H}$  NMR 400MHz DMSO- $d_6$  (Figure S19):**  $\delta$  (ppm) 7.76 (s, 4 H, aromatic protons).  **$^{19}\text{F}$  NMR 377 MHz, DMSO- $d_6$  (Figure S20):**  $\delta$  (ppm) -103.0.  **$^{13}\text{C}$  NMR 101 MHz, DMSO- $d_6$  (Figure S21):**  $\delta$  (ppm) 165.1 (RCOOR,  $J_{\text{C-F}} = 33$  Hz), 135.9 ( $\text{C}^{\text{V}}$  aromatic,  $J_{\text{C-F}} = 27$  Hz), 125.6 (CH aromatic,  $J_{\text{C-F}} = 168$  Hz), 113.5 ( $\text{CF}_2$ ,  $J_{\text{C-F}} = 250$  Hz), 40.0 (DMSO). **HRMS (ESI-)** Calc. for  $[\text{M}-\text{H}]^-$  265.0129, found 265.0135. **FTIR spectrum:** Figure S22.

**Synthesis of BDGE/P-DA reference material:** 0.97 g (10 meq ;  $\text{EEW}=97$  g/eq) of 1,4-phenylenediacetic acid was mixed with 1.19 g of BDGE at 90 °C to obtain a homogeneous light brown mixture. The mixture was cast in aluminum molds and left overnight in an oven at 120 °C. The mixture was not cured and a subsequent 1 h step at 180 °C was applied. The curing was checked by DSC and no remaining exothermic phenomenon was observed.

**Synthesis of BDGE/P-DAF vitrimer:** 1 g (7.5 meq COOH,  $\text{HEW}=133$ ) of P-DAF and 1.067 g (7.5 meq epoxy,  $\text{EEW}=142$ ) of butanediol diglycidyl ether (BDGE) were mixed together manually at room temperature until P-DAF was totally dissolved. A viscous clear yellowish solution was obtained and

quickly cast in PTFE molds. The solution was left to gel at room temperature, typically for 8 hours. Then, a brittle gel was obtained, unmolded and left for 3 h in an oven at 150 °C.

#### *Instrumentation*

**NMR:**  $^1\text{H}$ ,  $^{13}\text{C}$  and  $^{19}\text{F}$  were acquired on a Bruker Avance 400 MHz spectrometer at 23 °C. External reference was tetramethylsilane (TMS) with chemical shifts given in ppm. Samples were dissolved or diluted in 0.5 mL of  $\text{CDCl}_3$  or  $\text{DMSO-d}_6$  depending on their solubility.

**FTIR:** FTIR spectra were acquired on a ThermoScientific Nicolet iS50 FT-IR equipped with an attenuated total reflectance cell (ATR). The data were analyzed using the software OMNIC Series 8.2 from Thermo Scientific.

**HRMAS:** High resolution MAS NMR experiments were carried out on a Varian VNMRS 600 MHz spectrometer equipped with a wide bore magnet ( $B_0 = 14.1 \text{ T}$ ). Prior to HRMAS NMR experiments, the BDGE and the P-DAF were manually mixed together in a beaker, and injected in a 4 mm quartz zirconia HRMAS rotor insert with a 1 mL syringe. No solvent was added and the calibration was made using the peaks at 72 and 26 ppm of the BDGE, as observed in liquid NMR. Experiments were performed at room temperature. The sample spinning rate was 5 kHz.  $^{13}\text{C}$  NMR spectra were recorded at 20 °C, 38 kHz for spectral width, 15 kHz for transmitter frequency offset, 0.1 s for acquisition time, 256 scans (NS) with a 45 ° pulse (5.5  $\mu\text{s}$ ) and a relaxation delay at 1 s.  $^1\text{H}$  decoupling was applied during the whole sequence. The outstandingly short overall acquisition time compared to usual  $^{13}\text{C}$  experiments allowed to obtain spectra within a few minutes and to monitor qualitatively the polymerization reaction for several hours.

**Mechanical analysis:** Dynamic Mechanical Analyses were carried out on Metravib DMA 25 with Dynatest 6.8 software. Uniaxial stretching of samples ( $1 \times 2 \times 6 \text{ mm}^3$ ) was performed while heating at a rate of 3 °C  $\text{min}^{-1}$  from -90 °C to 150 °C, at a  $f=1 \text{ Hz}$  frequency. Relaxation experiments were performed on a ThermoScientific Haake Mars 60 rheometer equipped with a electric heating cell and a textured 8-mm plane-plane geometry. A 10 % torsional strain was applied on 8 mm diameter and 2 mm thickness circular samples, and the relaxation modulus evolution with time was monitored. The curing checking experiment was performed on a TA Ares G2 at a given temperature (150 or 170 °C) by applying a 0.1 % deformation at  $\omega = 1 \text{ rad}\cdot\text{s}^{-1}$  under a normal force of 100 grams every 2 minutes, and monitoring  $G'$ .

**TGA:** Thermogravimetric thermograms were recorded on a TA TGA G50 appliance using a 40  $\text{mL min}^{-1}$  flux of synthetic air as purge gas. Approximately 10 mg of sample were used for each analysis. Ramps from 20 to 500 °C were applied at a rate of 20 °C  $\text{min}^{-1}$ .

**DSC:** Analyses were carried out using a NETZSCH DSC200F3 calorimeter. The calibration was performed using adamantane, biphenyl, indium, tin, bismuth and zinc standards. Nitrogen was used as purge gas. Approximately 10 mg of sample were placed in perforated aluminum pans and the thermal properties were recorded between -100 °C and the temperature of 2% mass loss  $T_{d2\%}$  at 20 °C  $\text{min}^{-1}$ . The reported values are the values measured during the second heating ramp.

**Reprocessing:** the material was cut into  $1 \times 1 \times 1 \text{ mm}^3$  pieces and then pressed in a PTFE mold for 1.5 h at 150 °C under a 6 tons load using a Carver 3960 manual heating press.

#### *Conflicts of interest*

There are no conflicts to declare.

## Acknowledgements

This work was funded by the Institut Carnot Chimie Balard CIRIMAT (16CARN000801). The authors would like to thank Dr. Marc Guerre and Dr. François Tournilhac for fruitful discussions.

## References

- 1 J.-P. Pascault, H. Sautereau, J. Verdu and R. J. J. Williams, *Thermosetting Polymers*, Marcel Dekker, Inc., New York, 2002.
- 2 S. J. Pickering, in *Wiley Encyclopedia of Composites*, John Wiley & Sons, Inc., Hoboken, New Jersey, 2012.
- 3 L. Leibler, M. Rubinstein and R. H. Colby, *Macromolecules*, 2002, **24**, 4701–4707.
- 4 C. J. Kloxin, T. F. Scott, B. J. Adzima and C. N. Bowman, *Macromolecules*, 2010, **43**, 2643–2653.
- 5 C. N. Bowman and C. J. Kloxin, *Angew. Chemie - Int. Ed.*, 2012, **51**, 4272–4274.
- 6 C. J. Kloxin and C. N. Bowman, *Chem. Soc. Rev.*, 2013, **42**, 7161–7173.
- 7 X. Chen, M. A. Dam, K. Ono, A. Mal, H. Shen, S. R. Nutt, K. Sheran and F. Wudl, *Science (80-. )*, 2002, **295**, 1698–1702.
- 8 V. Froidevaux, M. Borne, E. Laborbe, R. Auvergne, A. Gandini and B. Boutevin, *RSC Adv.*, 2015, **5**, 37742–37754.
- 9 A. Gandini, *Prog. Polym. Sci.*, 2013, **38**, 1–29.
- 10 Q.-A. Poutrel, J. J. Blaker, C. Soutis, F. Tournilhac and M. Gresil, *Polym. Chem.*, 2020, **11**, 5327–5338.
- 11 T. F. Scott, A. D. Schneider, W. D. Cook and C. N. Bowman, *Science (80-. )*, 2005, **308**, 1615–1617.
- 12 D. Montarnal, M. Capelot, F. Tournilhac and L. Leibler, *Science (80-. )*, 2011, **334**, 965–968.
- 13 R. L. Snyder, D. J. Fortman, G. X. De Hoe, M. A. Hillmyer and W. R. Dichtel, *Macromolecules*, 2018, **51**, 389–397.
- 14 M. Röttger, T. Domenech, R. Van Der Weegen, A. Breuillac, R. Nicolaÿ and L. Leibler, *Science (80-. )*, 2017, **356**, 62–65.
- 15 F. Caffy and R. Nicolaÿ, *Polym. Chem.*, 2019, **10**, 3107–3115.
- 16 Y.-X. Lu and Z. Guan, *J. Am. Chem. Soc.*, 2012, **134**, 14226–14231.
- 17 W. Denissen, M. Droesbeke, R. Nicolaÿ, L. Leibler, J. M. Winne and F. E. Du Prez, *Nat. Commun.*, 2017, **8**, 14857.
- 18 W. Denissen, G. Rivero, R. Nicolaÿ, L. Leibler, J. M. Winne and F. E. Du Prez, *Adv. Funct. Mater.*, 2015, **25**, 2451–2457.
- 19 M. Guerre, C. Taplan, R. Nicolaÿ, J. M. Winne and F. E. Du Prez, *J. Am. Chem. Soc.*, 2018, **140**, 13272–13284.
- 20 H. Zhang, D. Wang, W. Liu, P. Li, J. Liu, C. Liu, J. Zhang, N. Zhao and J. Xu, *J. Polym. Sci. Part A Polym. Chem.*, 2017, **55**, 2011–2018.
- 21 S. Wang, S. Ma, Q. Li, X. Xu, B. Wang, K. Huang, Y. Liu and J. Zhu, *Macromolecules*, 2020, **53**,

- 2919–2931.
- 22 H. Zheng, Q. Liu, X. Lei, Y. Chen, B. Zhang and Q. Zhang, *J. Mater. Sci.*, 2019, **54**, 2690–2698.
- 23 R. Hajj, A. Duval, S. Dhers and L. Avérous, *Macromolecules*, 2020, **53**, 3796–3805.
- 24 M. Capelot, M. M. Unterlass, F. Tournilhac and L. Leibler, *ACS Macro Lett.*, 2012, **1**, 789–792.
- 25 J. Wang, S. Chen, T. Lin, J. Ke, T. Chen, X. Wu and C. Lin, *RSC Adv.*, 2020, **10**, 39271–39276.
- 26 J. J. Lessard, L. F. Garcia, C. P. Easterling, M. B. Sims, K. C. Bentz, S. Arencibia, D. A. Savin and B. S. Sumerlin, *Macromolecules*, 2019, **52**, 2105–2111.
- 27 C. He, S. Shi, D. Wang, B. A. Helms and T. P. Russell, *J. Am. Chem. Soc.*, 2019, **141**, 13753–13757.
- 28 J. Han, T. Liu, C. Hao, S. Zhang, B. Guo and J. Zhang, *Macromolecules*, 2018, **51**, 6789–6799.
- 29 T. Liu, S. Zhang, C. Hao, C. Verdi, W. Liu, H. Liu and J. Zhang, *Macromol. Rapid Commun.*, 2019, **40**, 1800889.
- 30 F. I. Altuna, V. Pettarin and R. J. J. Williams, *Green Chem.*, 2013, **15**, 3360–3366.
- 31 F. I. Altuna, C. E. Hoppe and R. J. J. Williams, *Eur. Polym. J.*, 2019, **113**, 297–304.
- 32 F. Cuminet, S. Caillol, É. Dantras, É. Leclerc and V. Ladmiraal, *Macromolecules*, 2021, **54**, 3927–3961.
- 33 S. Lemouzy, F. Cuminet, D. Berne, S. Caillol, V. Ladmiraal, R. Poli, E. Leclerc, S. Lemouzy, F. Cuminet, D. Berne, S. Caillol, V. Ladmiraal, E. Leclerc and R. Poli, *Chem. – A Eur. J.*, , DOI:10.1002/CHEM.202201135.
- 34 F. Cuminet, D. Berne, S. Lemouzy, E. Dantras, C. Joly-Duhamel, S. Caillol, E. Leclerc and V. Ladmiraal, *Polym. Chem.*, 2022, **8**, 5255–5446.
- 35 D. Berne, F. Cuminet, S. Lemouzy, C. Joly-Duhamel, R. Poli, S. Caillol, E. Leclerc and V. Ladmiraal, *Macromolecules*, 2022, **55**, 1669–1679.
- 36 B. Steinmann, *Polym. Bull.*, 1989, **22**, 637–644.
- 37 H. Eto, Y. Kaneko and T. Sakamoto, *Chem. Pharm. Bull.*, 2000, **48**, 982–990.
- 38 S. Mizuta, I. S. R. Stenhagen, M. O’Duill, J. Wolstenhulme, A. K. Kirjavainen, S. J. Forsback, M. Tredwell, G. Sandford, P. R. Moore, M. Huiban, S. K. Luthra, J. Passchier, O. Solin and V. Gouverneur, *Org. Lett.*, 2013, **15**, 2648–2651.
- 39 Y. Liu, S. Ma, Q. Li, S. Wang, K. Huang, X. Xu, B. Wang and J. Zhu, *Eur. Polym. J.*, 2020, **135**, 109881.
- 40 J. Han, T. Liu, S. Zhang, C. Hao, J. Xin, B. Guo and J. Zhang, *Ind. Eng. Chem. Res.*, 2019, **58**, 6466–6475.